

Nuclear spin relaxation rates in two-leg spin ladders

F. Naef and Xiaoqun Wang

*Institut Romand de Recherche Numérique en Physique des Matériaux (IRRMA),
INR-Ecublens, CH-1015 Lausanne, Switzerland*

Using the transfer-matrix DMRG method, we study the nuclear spin relaxation rate $1/T_1$ in the two-leg $s=1/2$ ladder as function of the inter-chain (J_\perp) and intra-chain (J_\parallel) couplings. In particular, we separate the $q_y = 0$ and π contributions and show that the later contribute significantly to the copper relaxation rate $^{63}(1/T_1)$ in the experimentally relevant coupling and temperature range. We compare our results to both theoretical predictions and experimental measures on ladder materials.

76.60.-k, 75.10.Jm, 75.40.Gb

Dynamical properties, while providing the most detailed information on the physics of low-dimensional antiferromagnets are also the most difficult for theoretical predictions. Measured in NMR experiments probing the low-frequency spin dynamics, they continue to reveal unexpected features. For instance, the recent experiments by Imai *et al.* [1] on the Cu_2O_3 two-leg $s=1/2$ ladders in $\text{La}_6\text{Ca}_8\text{Cu}_{24}\text{O}_{41}$ have shown the different temperature T dependence of the nuclear spin relaxation rate $1/T_1$ for the oxygen ($^{17}(1/T_1)$) and copper ($^{63}(1/T_1)$) atoms. Although both exhibit activated behavior below $T \simeq 350$ K, $^{63}(1/T_1)$ shows a crossover to a linear T dependence above $T \simeq 350$ K. Shortly after these experiments were performed, Ivanov and Lee [2] proposed that the crossover may be understood from the momentum transfer $\mathbf{q} = (\pi, \pi)$ contributions in the weakly coupled chain limit. The importance of the $q_y = \pi$ processes was also mentioned earlier by Sandvik *et al.* [3] in a study of $^{63}(1/T_1)$ for SrCu_2O_3 , where they consider the isotropic ladder at $T/J \geq 0.2$. Despite these findings, a better theoretical understanding of $1/T_1$ in isolated ladders is necessary, as emphasized in Refs. [1,2].

Our purpose is to determine $1/T_1$ for the experimentally relevant ratio of inter (J_\perp) and intra-chain (J_\parallel) couplings, separating the $q_y = 0$ and π contributions. We will use the transfer-matrix density-matrix renormalization group for the evaluation of thermodynamic properties [4] and local imaginary time correlations [5,6] of one-dimensional tight-binding models. Combined with an analytical continuation, this technique has recently proven to provide reliable real frequency correlations down to low temperatures [6]. In the low- T regime, our results show a good agreement to analytical results obtained in the weak or strong coupling limits [2,7]. At higher T , we demonstrate the importance of the $(1/T_1)_\pi$ contributions to $^{63}(1/T_1)$ experiments, in particular, our result reproduces the crossover to the linear paramagnetic regime observed in the $^{63}(1/T_1)$ rate.

The most recent estimates of J_\parallel/J_\perp from susceptibility and neutron scattering experiments agree for a value of about 0.5 [8,9]. On the other hand, estimating J_\parallel/J_\perp from NMR rates, we found that the standard ladder, together with the hyperfine couplings measured in Refs.

[1,13], are unable to account for $J_\parallel/J_\perp \sim 0.5$ but favors $J_\parallel/J_\perp \sim 1$.

The two-leg ladder is described by the antiferromagnetic Heisenberg Hamiltonian

$$H = \sum_{i=1}^N J_\parallel (\mathbf{S}_{1,i} \cdot \mathbf{S}_{1,i+1} + \mathbf{S}_{2,i} \cdot \mathbf{S}_{2,i+1}) + J_\perp \mathbf{S}_{1,i} \cdot \mathbf{S}_{2,i}, \quad (1)$$

where $\mathbf{S}_{n,i}$ denotes a $s=1/2$ spin operator at the i -th rung and the n -th chain. It is by now well established that the spectrum of the Hamiltonian (1) consists of an $S=0$ ground state, the lowest-lying excited states forming a gaped $S=1$, $k_y = \pi$ single magnon branch with minimum Δ at $k_x = \pi$ [7,10,11].

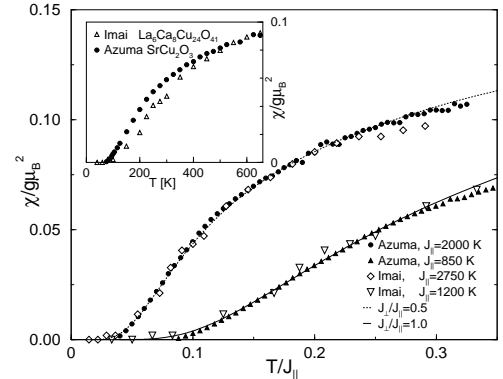


FIG. 1. Comparison of the susceptibility and Knight shifts to transfer-matrix DMRG results for $J_\parallel/J_\perp = 0.5$ and 1. Inset: susceptibility and Knight shift measurements compared.

The issue of determining the values of J_\parallel and J_\perp has raised some controversy, indeed estimates from various authors [1,12,13,8,14] range from $J_\perp/J_\parallel \simeq 0.5$ to 1, with an emerging consensus for about 0.5. Fitting our numerical results to susceptibility [12] and Knight shift [1] experiments, we confirm in Fig. 1 that the best agreement is found when $J_\perp/J_\parallel = 0.5$ for SrCu_2O_3 [15], implying energy scales $\Delta \simeq 420\text{K}$ and $J_\parallel \simeq 2000\text{K}$. Nevertheless, a reasonable fit to $J_\perp/J_\parallel = 1$ is also possible in a slightly narrower T -range, showing that the susceptibility is relatively insensitive to J_\perp/J_\parallel at low- T . Moreover, we point out in the inset that the susceptibility and Knight shift measurements are not fully consistent through the

entire T -range, implying material-dependent J_{\parallel} values. In principle, Knight shifts are better suited for a comparison with theoretical results, since they involve no subtraction of a Curie term and no unknown g factor [12,8].

The nuclear relaxation rate $1/T_1$ is given by

$$b\left(\frac{1}{T_1}\right) = \sum_{q_y=0,\pi} \int {}^bF(\mathbf{q})S(\mathbf{q},\omega_N) dq_x, \quad b = 63, 17 \quad (2)$$

$$S(\mathbf{q},\omega) = \frac{1}{2N} \sum_{i,j,m,n} \int \langle S_{n,i}^z(t)S_{m,j}^z \rangle e^{i\mathbf{q}\cdot(j-i,m-n)+\omega t} dt .$$

Here, ω_N is the nuclear Larmor frequency and ${}^bF(\mathbf{q})$ are the appropriate hyperfine couplings. According to Ref. [1], ${}^{63}F(\mathbf{q}) = A^2$ for ${}^{63}\text{Cu}$, and ${}^{17}F_2(\mathbf{q}) = 4F^2 \cos^2(q_y/2)$ for the rung $O(2)$ oxygen atoms [16]. Contrary to CuO_2 planes, it has been argued that considering only a local hyperfine interaction for the ${}^{63}\text{Cu}$ nucleus in ladders [3,13] is sufficient.

To determine $1/T_1$, the transfer-matrix DMRG method permits a very precise evaluation of the imaginary time Green's function [6]

$$G(\tau) = \langle S_{1,1}^z(\tau)S_{m,j}^z \rangle \quad (3)$$

where $S_{n,i}^z(\tau) = e^{\tau H} S_{n,i}^z e^{-\tau H}$ and the indices $(m,j) \in \{(1,1), (2,1), (1,2), (2,2)\}$ run over the four corners of a plaquette. For all calculations, we chose an imaginary time slice $\epsilon = 0.025/J_{\parallel}$ and $m = 200$ states were kept to represent the transfer-matrix. After an analytical continuation using the Maximum Entropy method, we can resolve $S(\mathbf{q},\omega)$ in $q_y = 0$ or π and obtain the averages over the q_x momentum transfer:

$$\bar{S}_0(q_y,\omega) = \frac{1}{4\pi} \int dq_x \cos^2(q_x/2)S(q_x,q_y,\omega)$$

$$\bar{S}_{\pi}(q_y,\omega) = \frac{1}{4\pi} \int dq_x \sin^2(q_x/2)S(q_x,q_y,\omega) . \quad (4)$$

As indicated by the notation, $\bar{S}_0(q_y,\omega)$ ($\bar{S}_{\pi}(q_y,\omega)$) is dominated by processes with q_x close to 0 (π). For the hyperfine couplings given above, the copper and oxygen rates are fully determined by appropriate combinations of $\bar{S}_{\bar{q}_x}(q_y,\omega)$, $\bar{q}_x = 0, \pi$. Accordingly, we also define

$$\left(\frac{1}{T_1}\right)_{q_y} = \bar{S}_0(q_y,\omega_N) + \bar{S}_{\pi}(q_y,\omega_N) , \quad (5)$$

the dimensionless contributions to $1/T_1$ from the $q_y = 0, \pi$ momentum space sectors.

For illustration, we show in Fig. 2 $\bar{S}_{\bar{q}_x}(q_y,\omega)$ for the case $J_{\perp}/J_{\parallel}=1$ as a function of T . As the latter drops, we can see clearly the signatures of the low-lying spectrum emerging. Indeed, the main peak is due to excitations from the ground state to the single magnon branch for the $q_y=\pi$ sector and to the 2-magnon continuum for $q_y=0$, for instance, it appears correctly from $\bar{S}_{\pi}(\pi,\omega)$ that the

minimum gap approaches the $T=0$ value $\Delta=0.502$. Such contributions to $\bar{S}_{\bar{q}_x}(q_y,\omega)$ become T independent for $T \rightarrow 0$, however, they do not contribute to $1/T_1$ as they all involve frequencies $\omega \geq \Delta \gg \omega_N$ (≈ 3 mK). On the contrary, there are thermally activated contributions to $1/T_1$, as they involve excitations for $\omega \rightarrow 0$ [17]. As seen in Fig. 2, this limit is dominated in the low- T regime by processes with $(\bar{q}_x, q_y) = (0, 0)$ and (π, π) .

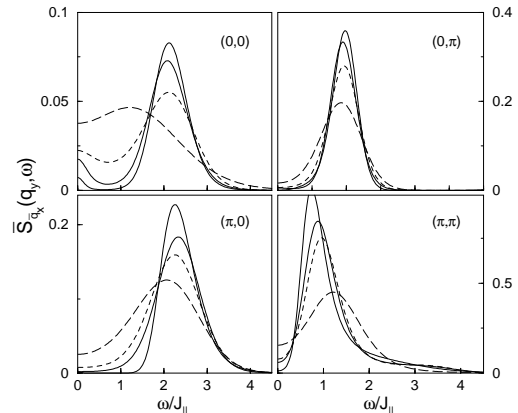


FIG. 2. $\bar{S}_{\bar{q}_x}(q_y,\omega)$ for $J_{\perp}/J_{\parallel}=1$. $T/J_{\parallel}=1/2$ (dotted line), $1/3$ (dashed), $1/4$ (thin) and $1/6$ (thick).

The first contributions involve two thermally excited magnons near the minimum of the branch $e(k_x, k_y=\pi)=\Delta+a(k_x-\pi)^2$, according to Ref. [7], they lead to

$$\left(\frac{1}{T_1}\right)_0 \propto \frac{1}{a} e^{-\Delta/T} [0.809 - \ln(\frac{\omega_N}{T})] . \quad (6)$$

Corrections to the quadratic minimum [18] only change the prefactor of the exponential term slightly for $T/\Delta \lesssim 0.3$. The logarithmic divergence in Eq.(6) cannot be resolved by the Maximum Entropy method, however, it does not change the dominant exponential behavior. For instance, the factor in the square brackets changes only by about 5 percent from $T = \Delta/2$ to $\Delta/4$.

The second important contributions with $q_y = \pi$ involve scattering of single magnons with the 2-magnon continuum. By representing the low-lying excitations in terms of free massive fermions [11] in the weakly coupled chain limit, it was proposed in Ref. [2] that

$$\left(\frac{1}{T_1}\right)_{\pi} \propto \left(\frac{T}{\Delta}\right) e^{-2\Delta/T} . \quad (7)$$

As the scale 2Δ corresponds to the bottom of the 2-magnon continuum at $\mathbf{k} = (0,0)$ independent of J_{\perp}/J_{\parallel} [10,19], this result should hold over a wider coupling range. In fact, exact diagonalisation (ED) results show the existence of large matrix elements $|\langle n|S_q^z|m \rangle|^2$ between the 2-magnon continuum at $\mathbf{k} = (0,0)$ and the single magnon branch. Such processes are characterized by a momentum transfer q_x which rapidly shifts close to

π with decreasing J_{\perp} . From the analysis of the spectrum [10], it follows that $q_x/\pi \approx 0.5, 0.8$ and 0.95 for $J_{\perp}/J_{\parallel} = 2, 1$ and 0.5 . Other important $q_y = \pi$ processes occur between the single magnon branch at $\mathbf{k}=(0, \pi)$ and the continuum near $\mathbf{k}=(\pi, 0)$ when $J_{\perp}/J_{\parallel} \lesssim 0.5$. However, these have a larger activation gap of about 3.7Δ .

Let us first discuss our results for $1/T_1$ as a function of J_{\perp} and T . We should point out that the values $\bar{S}_{q_x}(q_y, \omega \rightarrow 0)$ become very small compared to the magnitude of the main peak as T is lowered. Therefore, for a reliable estimate of $1/T_1$, it is essential, (i) to work with very precise imaginary time data, and (ii) to separate the different \mathbf{q} space contributions, as the integrated weight of the $q_y = 0$ and π sectors differ considerably. In Fig. 3, we present $(1/T_1)_0$ and $(1/T_1)_{\pi}$ in the low- T regime, where T is scaled by the spin gap Δ .

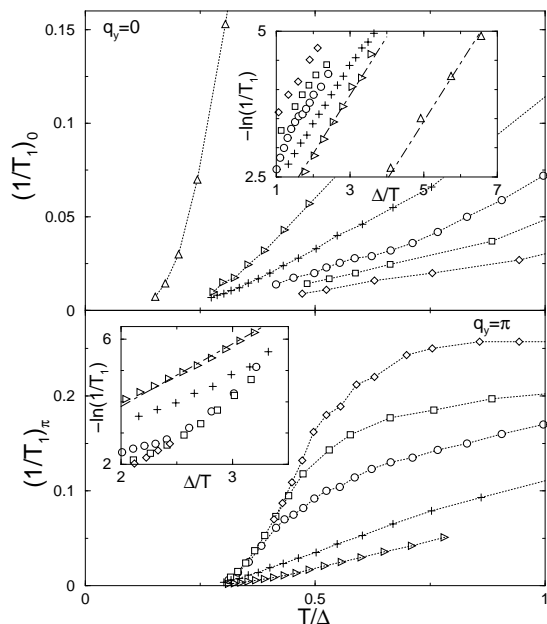


FIG. 3. Low- T behavior of $(1/T_1)_0$ and $(1/T_1)_{\pi}$ for $J_{\perp}/J_{\parallel} = 5$ (Δ), 2 (\triangleright), 1.5 ($+$), 1 (\circ), 0.8 (\square) and 0.6 (\diamond). Insets: The dot-dashed lines have slopes 1 (2) for $q_y=0$ (π).

$(1/T_1)_0$ shows the correct behavior of Eq.(6), especially for large J_{\perp}/J_{\parallel} , when low enough T/Δ can be reached to clearly identify the activated regime. This is verified in the inset where we have plotted a line of slope one on a logarithmic scale. We also observe that the prefactor of the exponential strongly depends on J_{\perp}/J_{\parallel} , consistently with the factor $1/a$ in Eq.(6). Indeed, as the dispersion of the single magnon branch flattens with increasing J_{\perp} , $1/a$ grows and $\lim_{J_{\perp} \rightarrow \infty} 1/a = \infty$ [7,10]. The $q_y = \pi$ results reveal a larger gap which can be fitted consistently to Eq.(7) when $J_{\perp}/J_{\parallel} = 1.5, 2$ (see inset). When $J_{\perp}/J_{\parallel} \lesssim 1$, we find some deviations from Eq.(7) In this regime, the low- T extraction of $(1/T_1)_{\pi}$ becomes more delicate as the growing main frequency peak near $\omega = \Delta$ (due to excitations from the ground state to the single

magnon branch) may bias the limit $S(\mathbf{q}, \omega \rightarrow 0)$ (see Fig. 2). On the other hand, we cannot exclude that the above mentioned processes with a gap $\approx 3.7\Delta$ contribute significantly at our lowest temperatures. For the case $J_{\perp}/J_{\parallel} = 5$ (not shown in Fig. 3), $(1/T_1)_{\pi} = 0$ since the single magnon band and the 2-magnon continuum do not yet overlap.

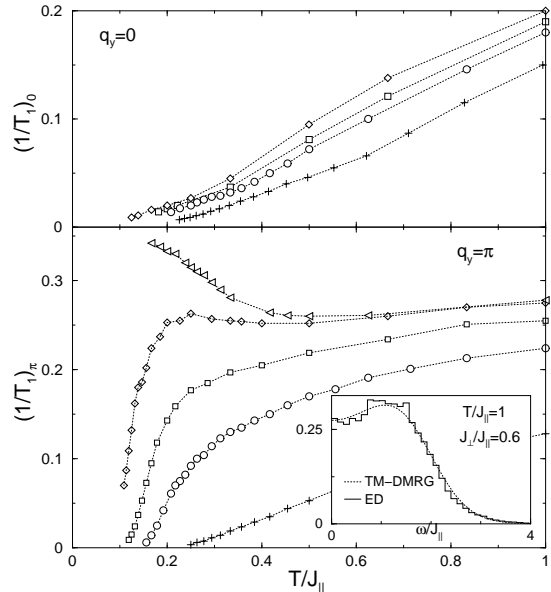


FIG. 4. $(1/T_1)_0$ and $(1/T_1)_{\pi}$ as function of T/J_{\parallel} for $J_{\perp}/J_{\parallel} = 1.5$ ($+$), 1 (\circ), 0.8 (\square), 0.6 (\diamond) and 0.4 (\triangleleft). Inset: comparison of $S(0, \pi, \omega) + S(\pi, \pi, \omega)$ from ED and Transfer-Matrix DMRG.

A wider T range is shown in Fig. 4. $(1/T_1)_{\pi}$ obtained at $T/J_{\parallel} = 1$ agree within 5 percent with those from ED of an 8-rung ladder, as seen in the inset for $J_{\perp}/J_{\parallel} = 0.6$. However, due to finite size effects, the determination of $1/T_1$ from ED becomes meaningless below $T/J_{\parallel} \simeq 0.8$.

As $(1/T_1)_0$ obeys a predominantly linear intermediate to high- T behavior for all J_{\perp} above $T \simeq 0.4 J_{\parallel}$, $(1/T_1)_{\pi}$ exhibits a qualitative change as J_{\perp}/J_{\parallel} is decreased. Indeed, for $J_{\perp}/J_{\parallel} \leq 0.6$ $(1/T_1)_{\pi}$ develops a maximum near $T/J_{\parallel} \sim 0.2$ becoming sharper with decreasing inter-chain coupling. We believe such a feature is reminiscent of the weak coupling limit, as our $(1/T_1)_{\pi}$ for $J_{\perp}/J_{\parallel} \leq 0.6$ shows a good agreement to the behavior predicted in Ref. [2]. There, Ivanov and Lee also argued that with increasing T , $(1/T_1)_{\pi}$ flattens to the single Heisenberg chain result [20], as we observe for $J_{\perp}/J_{\parallel} = 0.4$ and 0.6 above $T/J_{\parallel} = 0.4$. In spite of the larger gap, we find that $(1/T_1)_{\pi}$ dominates over $(1/T_1)_0$ in a wide intermediate- T regime as can be verified from Figs. 3 and 4. For instance, when $T/\Delta = 1$, $(1/T_1)_{\pi}$ exceeds $(1/T_1)_0$ by a factor 2.5 (resp. 9) for $J_{\perp}/J_{\parallel} = 1$ (resp. 0.6). In particular, for $J_{\perp}/J_{\parallel} = 1$, we observe the crossing of $(1/T_1)_{\pi}$ and $(1/T_1)_0$ at $T/\Delta \simeq 0.35$. This consideration implies that both $q_y = 0$ and π contributions are relevant to cop-

per $^{63}(1/T_1)$ experiments above $T \simeq 0.35 \Delta$ (typically ≈ 200 K in Cu_2O_3 ladders). In fact, taking into account the usually omitted $q_y = \pi$ processes to fit the low- T $^{63}(1/T_1)$ data of Ishida *et al.* [13] on SrCu_2O_3 , we obtain for T between 100 and 300 K a gap $\Delta \approx 520$ K, while considering only the form for $(1/T_1)_0$ leads to $\Delta \approx 700$ K. Hence, the discrepancy between estimates of the gap from $^{63}(1/T_1)$ and susceptibility [12,13] (leading to $\Delta \simeq 420$ K) is reduced.

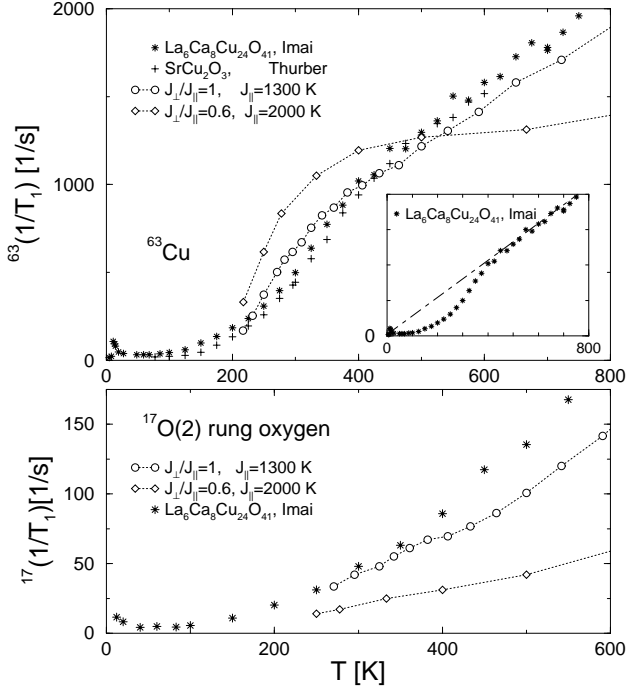


FIG. 5. Comparison of NMR rates in SrCu_2O_3 [21] and $\text{La}_6\text{Ca}_8\text{Cu}_{24}\text{O}_{41}$ [1] to numerical results. Inset: Imai's data, the high- T regime extrapolates to zero.

Let us now compare our results with experimental measurements of $^{63}(1/T_1)$ and the rung oxygen $^{17}(1/T_1)$ rate in SrCu_2O_3 and $\text{La}_6\text{Ca}_8\text{Cu}_{24}\text{O}_{41}$. To convert our values to the experimental unit, we considered the hyperfine couplings given in Ref. [13] for the ^{63}Cu and in Ref. [1] for the ^{17}O nuclei, so that the remaining free parameters are only J_\perp and J_\parallel , which we have chosen according to those obtained from the susceptibility fits in Fig. 1. Considering that T scales proportionally and $1/T_1$ inversely proportional to J_\parallel , we found good overall magnitudes, however, the precise T -dependence is not reproduced very accurately. Our results tend to indicate that $J_\perp/J_\parallel \sim 1$, in disagreement with $J_\perp/J_\parallel \sim 0.5$ from the susceptibility. Especially, the ‘linear’ high- T behavior of $^{63}(1/T_1)$ extrapolating to zero (inset) cannot be reproduced with a smaller ratio J_\perp/J_\parallel .

These observations raise two important issues about ladder materials. First, the hyperfine couplings measured in Refs. [1,13] may not be sufficient for a quantitative discussion of NMR experiments within the standard lad-

der model. A possible improvement may be to consider transferred fields $^{63}F \propto (1 + 2r \cos q_x)^2 + r' \cos^2(q_y/2)$ on the copper atom, which can suppress the (π, π) -fluctuations by large factors [22] and favor a smaller ratio J_\perp/J_\parallel . This suggests that a better knowledge of the hyperfine couplings in ladder materials is needed for a quantitative interpretation of measured NMR data. Second, small corrections to the standard ladder such as interladder or frustration couplings are known to have little effect on bulk properties such as the spin gap [23]. Therefore, the accessible susceptibility measurements ($T/\Delta \lesssim 1$) are relatively insensitive to such corrections. On the other hand, local dynamic properties as NMR rates can be more substantially affected.

To summarize, we have shown that our technique provides reliable NMR rates $1/T_1$ in the standard ladder over a wide temperature range. In particular, we demonstrated that the $q_y = \pi$ contributions are crucial for understanding the crossover observed in $^{63}(1/T_1)$ experiments. Finally, we point out how quantitative results can indicate inconsistencies in estimates of J_\perp/J_\parallel from susceptibility and NMR measurements.

We thank X. Zotos and M. Long for helpful suggestions, T. Imai for kindly providing us the experimental measurements, D. C. Johnston and T. Xiang for useful communications. Our work was supported by the Swiss National Foundation grant no. 20-49486.96.

-
- [1] T. Imai, K.R. Thurber, K.M. Shen, A.W. Hunt and F.C. Chou, Phys. Rev. Lett. **81** 220 (1998).
 - [2] D. A. Ivanov and P. A. Lee, Phys. Rev. B **59**, 4803 (1999).
 - [3] A. W. Sandvik, E. Dagotto and D. J. Scalapino, Phys. Rev. B **53**, R2934 (1996).
 - [4] X. Wang and T. Xiang, Phys. Rev. B **56**, 56 (1997).
 - [5] T. Mutou, N. Shibata and K. Ueda, Phys. Rev. Lett. **81**, 4939 (1998).
 - [6] F. Naef, X. Wang, X. Zotos, and W. von der Linden, Phys. Rev. B **60**, 359 (1999); X. Wang, K. Hallberg and F. Naef in *Density-Matrix Renormalization*, Lecture Notes in Physics vol. 528, edited by I. Peschel, X. Wang, M Kaulke, and K. Hallberg, (Springer-Verlag, New York, 1999).
 - [7] M. Troyer, H. Tsunetsugu and D. Würtz, Phys. Rev. B **50**, 13 515 (1994).
 - [8] D. C. Johnston, Phys. Rev. B **54**, 13 009 (1996).
 - [9] R. S. Eccleston, M. Uehara, J. Akimitsu, H. Eisaki, N. Motoyama, and S. Uchida, Phys. Rev. Lett. **81**, 1702 (1998).
 - [10] T. Barnes and J. Riera, Phys. Rev. B **50**, 6817 (1994).
 - [11] D. G. Shelton, A. A. Neresyan and A. M. Tsvelik, Phys. Rev. B **53**, 8521 (1996).
 - [12] M. Azuma, Z. Hiroi, and M. Takano, Phys. Rev. Lett. **73** 3463 (1994).
 - [13] K. Ishida *et al.*, Phys. Rev. B **53** 2827 (1996).
 - [14] T. F. A. Müller, V. Anisimov, T. M. Rice, I. Dasgupta and T. Saha-Dasgupta, Phys. Rev. B **57** R12665 (1998).

- [15] D. C. Johnston, private communication.
- [16] We have absorbed constants in the hyperfine couplings, the link to Ref. [1] is given by: $A^2 = {}^{63}\gamma_N^2/\mu_B^2\hbar(A_a^2+A_b^2)$, $G^2 = {}^{17}\gamma_N^2/\mu_B^2\hbar(G_a^2+G_b^2)$ when $G = C, D, F$.
- [17] For all estimates of $1/T_1$, we consider $\bar{S}_{\bar{q}_x}(q_y, \omega \rightarrow 0)$.
- [18] R. Melzi and P. Carretta, cond-mat/9904074.
- [19] X. Wang, in preparation.
- [20] S. Sachdev, Phys. Rev. B **50**, 13 006 (1994).
- [21] K. R. Thurber, T. Imai, T. Saitoh, M. Azuma and M. Takano, to be published.
- [22] For instance $r = +0.25, r' = 0$ suppresses $((1/T_1)_{\bar{q}_x=\pi}$ over $(1/T_1)_{\bar{q}_x=\pi}$ by a factor ~ 5 .
- [23] X. Wang, cond-mat/9803290